NATURAL CONVECTION IN A SQUARE CAVITY PARTIALLY FILLED WITH POROUS MEDIUM AND NANOFLUID USING BUONGIORNO'S MODEL

CHERIFA BENYGZER[1]*, MOHAMED BOUZIT[1], ABDERRAHEM MOKHEFI[12]

Abstract. Natural convection is investigated in a square cavity divided in three layers, nanofluid at the middle and the upper and lower parts for porous layer. The cavity is heated from the left and cold from the right at constant temperature T_h and T_c respectively. The side walls are well insulated. The Buongiorno's model was used to evaluate the distribution of nanoparticles and takes account the Brownian and thermophoresis motion. The governing equations are solved by the Galerkin finite element method. The governing parameters are Rayleigh ($10^3 \leq$ Ra $\leq 10^6$), porous layer thickness ($0.3 \leq L_p \leq 0.05$).The result shows that increasing buoyancy forces reinforce circulation flow in the nanofluid layer than the porous layer, the decrease effect of porous layer thickness improve considerably the convective heat transfer. The heat and mass transfer are enhanced.

Key words: natural convection, porous layer, panofluid, Buongiorno model, heat transfer.

1. INTRODUCTION

The porous medium has been a subject of intensive studies, its can improve significantly convective heat transfer inside cavities [1–3]. In many engineering applications, such as industrial heat radiators, heat exchanger design, cooling of micro-electronic devices, solar collector.

A natural convection in enclosure partially filled with a nanofluid and porous layer, has attired a significant number of researchers A. Alsabery *et al*. [4–5]. The studies of the horizontally partitioned cavity have been reported by many authors [6–12].

A.I. Alsabery *et al*. [13] have studied a natural Convection in an Inclined Trapezoidal Cavity Partly Filled with a Porous and nanofluid layers, they resulted that the heat transfer rate is affected by the inclination angle of the cavity variation

---

[1] LSIM Maritime Science and Engineering Laboratory, Faculty of Mechanical Engineering, University of Science and Technology of Oran, Mohamed Boudiaf , El Maouar, Bp 1505, Bir Eldjir 31000, Oran, Algeria

[2] L2ME Modeling and Experimentation Laboratory, Faculty of Sciences and Technology, Bechar University B.P.417, 08000, Bechar, Algeria, Algeria

Ro. J. Techn. Sci. − Appl. Mechanics, Vol. 68, N° 1, P. 91–107, Bucharest, 2023

DOI: 10.59277/RJTS-AM.2023.1.06

and by the porous layer increment. Several nanoparticles depicted a diversity improvement on the convection heat transfer [14].

Zehba A. S. Raizah, *et al*. [15] have proved that the heat transfer through the nanofluid porous layer was determined to be the best toward high rates of Darcy number, porosity, and volume fraction of nanofluid. The control of the natural convection in partially layered square cavity composed of porous and fluid layer and a conductive solid body have been analyzed by M. Ismael and Hassan S. Ghalib [16].

Poulikakos and Bejan [17] have chosen different permeability of porous layers in a vertical rectangular enclosure.

The heat transfer rate maintains its maximum value when S reaches the critical value (S = 0.3). Inside a superposed enclosure filled with composite porous-hybrid nanofluid layers using a local thermal nonequilibrium model [18] and the existence of the porous layer in a specified value can enhance the convective heat transfer [19].

The enhancement of natural convection is attained when the permeability (Da) of the porous medium is very low and the porous layer thickness is greater than 0.5 of natural convection inside a square composite vertically layered cavity [20] Muneer A. Ismael & Ali J. Chamkha.

For a low Rayleigh number, the largest porous layer thickness and the highest cavity orientation improve the thermal performance in inclined partially porous layered cavity filled with a Cu–water nanofluid [21]. The properties and the position of porous layer strongly influence the thermal behavior of the cavity [22].

The increase of Darcy number of the porous media with a low value of the non-uniform porous layer thickness enhance the convective heat transfer in the cavity [23].

The main effect of porous layers is to reduce the upwind flow and then to decrease the convective heat transfer have been proved by P. Le Breton *et al*. [24].

The increasein the portion of the clear flow part in the cavity enhances heat transfer due to better hybrid nanofluid circulation [25].

M. Ghalambaz *et al*. [26] have studied the natural convection heat transfer in a square cavity filled with porous media saturated with a nanofluid using the Buongiorno's nanofluid model. The nanofluid and porous media have both positive and negative influences on heat transfer, since they can weaken the convection and also strengthen the conduction. Consequently, optimal volume fraction and porous layer thickness exist for different conditions of Ra and Da in order to maximize the Nusselt number [27].

2. MATHEMATIC MODEL

The problem configuration is schematically illustrated in Fig. 1. It consists of 2D natural convection in a square cavity containing nanofluid and porous layers. H represents the height of the cavity, T_h and T_c are the hot and cold constant temperature at the left and right wall, respectively. The remaining horizontal walls are considered to be adiabatic. The flow is considered to be laminar, steady, and incompressible, the Buongiorno model is used.

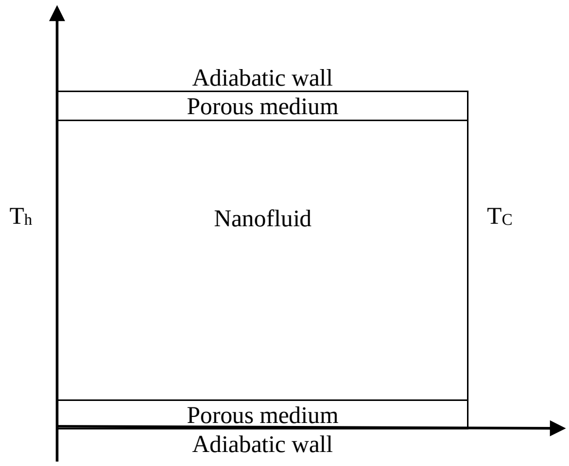

Fig. 1 – Physical problem studied.

The thermophysical properties of water and nanofluids are at 25°C.The configuration of the cavity and the flow is shown in Table 1.

Table 1

Thermophysical properties of water

Physical property	Water
C_p (J/kg)	4179
ρ (kg /m^3)	997.1
K (W/m k)	0.613
B (k^{-1})	21e-5
μ (kg/m s)	8.55e-4

The two-dimensional equations governing the stationary flow of nanofluids in natural convection inside a square cavity using Buongiorno mathematical model are described as follows

$$\frac{\partial \rho}{\partial t}+\rho\left(\frac{\partial u}{\partial x}+\frac{\partial v}{\partial y}\right)=0\,, \tag{1}$$

$$\rho\left(\frac{\partial u}{\partial t}+u\frac{\partial u}{\partial x}+v\frac{\partial u}{\partial y}\right)=-\frac{\partial p}{\partial x}+\mu\left(\frac{\partial^2 u}{\partial x^2}+\frac{\partial^2 u}{\partial y^2}\right)-\frac{\mu}{K}u\,, \tag{2}$$

$$\begin{aligned}&\rho\left(\frac{\partial v}{\partial t}+u\frac{\partial v}{\partial x}+v\frac{\partial v}{\partial y}\right)=-\frac{\partial p}{\partial y}+\mu\left(\frac{\partial^2 v}{\partial x^2}+\frac{\partial^2 v}{\partial y^2}\right)-\frac{\mu}{K}v+\\&+\left[\left(1-C_c\right)\rho_{\mathrm{f}}\left(T-T_c\right)\beta_{\mathrm{f}}-\left(C-C_c\right)\left(\rho_{\mathrm{s}}-\rho_{\mathrm{f}}\right)\right]g,\end{aligned} \tag{3}$$

$$\begin{aligned}&\frac{\partial T}{\partial t}+u\frac{\partial T}{\partial x}+v\frac{\partial T}{\partial y}=\alpha\left(\frac{\partial^2 T}{\partial x^2}+\frac{\partial^2 T}{\partial y^2}\right)+\\&+\delta\left\{D_B\left(\frac{\partial T}{\partial x}\frac{\partial C}{\partial x}+\frac{\partial T}{\partial y}\frac{\partial C}{\partial y}\right)+\frac{D_T}{D_C}\left[\left(\frac{\partial T}{\partial x}\right)^2+\left(\frac{\partial T}{\partial y}\right)^2\right]\right\},\end{aligned} \tag{4}$$

$$\frac{\partial C}{\partial t}+u\frac{\partial C}{\partial x}+v\frac{\partial C}{\partial y}=D_B\left(\frac{\partial^2 C}{\partial x^2}+\frac{\partial^2 C}{\partial y^2}\right)+\frac{D_B D_T}{D_C}\left(\frac{\partial^2 T}{\partial x^2}+\frac{\partial^2 T}{\partial y^2}\right), \tag{5}$$

$$D_B=\frac{K_b T_0}{3\pi d_{\mathrm{p}}\mu}, \tag{6}$$

$$D_T=\frac{\beta\mu C_0}{\rho_{\mathrm{f}}}\,. \tag{7}$$

For an incompressible flow, the density of the fluid is constant as a function of the spatial position ($\rho =$ constant), the mass equation simply becomes:

$$\frac{\partial u}{\partial x}+\frac{\partial v}{\partial y}=0\,. \tag{9}$$

To generalize the phenomenon, a set of dimensionless variables has been introduced. It is defined as follows:

$$\begin{gathered}\left(X,Y\right)=\frac{\left(x,y\right)}{H},\quad \left(U,V\right)=\frac{H\left(u,v\right)}{\alpha_{\mathrm{f}}},\quad \theta=\frac{T-T_c}{T_h-T_c},\\ \varphi=\frac{C-C_c}{C_h-C_c},\quad P=\frac{pH^2}{\rho_{\mathrm{f}}\alpha_{\mathrm{f}}^2}.\end{gathered} \tag{10}$$

By introducing these dimensionless variables into the dimensional equations we obtain:

$$\frac{\partial U}{\partial X}+\frac{\partial V}{\partial Y}=0\,, \tag{11}$$

$$\frac{\partial U}{\partial \tau}+U\frac{\partial U}{\partial X}+V\frac{\partial U}{\partial Y}=-\frac{\partial P}{\partial X}+\mathrm{Pr}\left(\frac{\partial^2 U}{\partial X^2}+\frac{\partial^2 U}{\partial Y^2}\right)-\frac{\mathrm{Pr}}{\mathrm{Da}}U, \tag{12}$$

$$\begin{gathered}\frac{\partial V}{\partial \tau}+U\frac{\partial V}{\partial X}+V\frac{\partial V}{\partial Y}=-\frac{\partial P}{\partial Y}+\mathrm{Pr}\left(\frac{\partial^2 V}{\partial X^2}+\frac{\partial^2 V}{\partial Y^2}\right)-\frac{\mathrm{Pr}}{\mathrm{Da}}V+\\ +\mathrm{Ra}\,\mathrm{Pr}\left(\theta-\mathrm{Nr}\varphi\right),\end{gathered} \tag{13}$$

$$\begin{gathered}\frac{\partial \theta}{\partial t}+U\frac{\partial \theta}{\partial X}+V\frac{\partial \theta}{\partial Y}=\frac{\partial^2 \theta}{\partial X^2}+\frac{\partial^2 \theta}{\partial Y^2}+\mathrm{Nb}\left(\frac{\partial \theta}{\partial X}\frac{\partial \varphi}{\partial X}+\frac{\partial \theta}{\partial Y}\frac{\partial \varphi}{\partial Y}\right)+\\ +\mathrm{Nt}\left[\left(\frac{\partial \theta}{\partial X}\right)^2+\left(\frac{\partial \theta}{\partial Y}\right)^2\right],\end{gathered} \tag{14}$$

$$\frac{\partial \varphi}{\partial t}+U\frac{\partial \varphi}{\partial X}+V\frac{\partial \varphi}{\partial Y}=\frac{1}{\mathrm{Le}}\left(\frac{\partial^2 \varphi}{\partial X^2}+\frac{\partial^2 \varphi}{\partial Y^2}\right)+\frac{\mathrm{Nt}}{\mathrm{LeNb}}\left(\frac{\partial^2 \theta}{\partial X^2}+\frac{\partial^2 \theta}{\partial Y^2}\right). \tag{15}$$

New parameters appear in the dimensionless equations: Prandtl number, Darcy number, Rayleigh number, buoyancy ratio, Brownian motion, thermophoresis and Lewis number

$$\mathrm{Pr}=\frac{\mu Cp}{k}\,, \tag{16}$$

$$\mathrm{Da}=\frac{K}{H^2}, \tag{17}$$

$$\mathrm{Ra}=\frac{(1-C_c)\beta_\mathrm{f}\, g\,(T_h-T_c)H^3}{\nu_\mathrm{f}\,\alpha_\mathrm{f}}, \tag{18}$$

$$\mathrm{Nr}=\frac{(C_h-C_c)(\rho_\mathrm{s}-\rho_\mathrm{f})}{(1-C_c)\beta_\mathrm{f}\rho_\mathrm{f}\,(T_h-T_c)}, \tag{19}$$

$$NB = \frac{\left(C_h - C_c\right) D_B \left(\rho Cp\right)_\mathrm{s}}{\alpha_\mathrm{f}\left(\rho Cp\right)_\mathrm{f}}, \tag{20}$$

$$NT = \frac{D_T}{T_c}\frac{\left(\rho Cp\right)_\mathrm{s}}{\left(\rho Cp\right)_\mathrm{f}}\frac{\left(T_h - T_c\right)}{\alpha_\mathrm{f}}, \tag{21}$$

$$\mathrm{Le} = \frac{\alpha_\mathrm{f}}{D_B}. \tag{22}$$

2.1. BOUNDARY CONDITION

The proposed problem is provides with boundary condition in the dimensionless form of the cavity walls. At $\tau = 0$ we have in the whole domain $U = 0,\ V = 0,\ \theta = 1$ and $\varphi = 1$ for $\tau > 0$;

– On the left wall: $U = 0,\ V = 0,\ \theta = 1$ and $N_B \partial x \theta + N_T \partial x \varphi = 0$;

– On the right wall: $U = 0,\ V = 0,\ \theta = 0$ and $N_B \partial x \theta + N_T \partial x \varphi = 0$;

– On the top wall: $\partial y U = 0,\ \partial y V = 0,\ \partial y \theta = 0$ and $\partial y \varphi = 0$;

– On the bottom wall: $\partial y U = 0,\ V = 0,\ \partial y \theta = 0$ and $\partial y \varphi = 0$.

The physical quantities of heat transfer are local and average Nusselt and Sherwood numbers respectively Nu_{loc}, Sh_{loc}, Nu_{avg}, Sh_{avg} are defined as below

$$\mathrm{Nu}_L = -\left.\frac{\partial\theta}{\partial X}\right|_{X=1}, \quad \mathrm{Sh}_L = -\left.\frac{\partial\varphi}{\partial X}\right|_{X=1}, \tag{23}$$

$$\mathrm{Nu}_{avg} = \int_0^1 -\frac{\partial\theta}{\partial X}\mathrm{d}Y, \quad \mathrm{Sh}_{avg} = \int_0^1 -\frac{\partial\varphi}{\partial X}\mathrm{d}Y. \tag{24}$$

3. NUMERICAL METHOD AND VALIDATION

The finite element method based on the Galerkin discretization scheme was used to solve the differential equations with boundary conditions. A triangular mesh appears more adequate. The convergence criterion is of the order of 1e-6 for each variable. The analysis of the different properties values (stream function, temperature, concentration and average Nusselt and Sherwood number) are obtained for several meshes with a total number of elements of 26 394.

Table 2

Mesh grid analysis for the present configuration

Elmts	7802	15256	26394	51248	84670
Time	337 s	687 s	1158 s	30114 s	69150 s
Ψ	10.13993	10.14947	10.15307	10.15632	10.15770
T	0.50072	0.50071	0.50072	0.50071	0.50071
C	0.99606	0.99942	0.99894	1.00004	0.99917
Nu	4.64108	4.64333	4.64439	4.64570	4.64616
Sh	4.64110	4.64334	4.64439	4.64570	4.64616

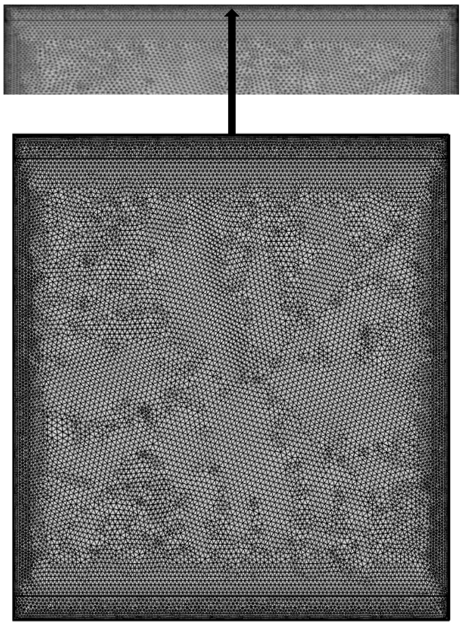

Fig. 2 – Grid mesh.

The validation of the reference geometry is used by de Sheikhzadeh, Nazari [28] was done under the same conditions, the equations used were similar and we can conclude that the same results are obtained for the iso-concentrations cases.

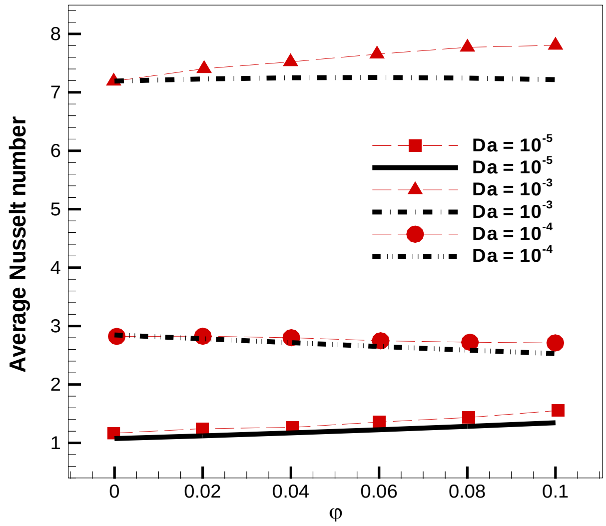

Fig. 3 – Numerical comparison results of average Nusselt number with Sheikhzadeh, Nazari.

4. RESULTS AND DISCUSSION

The numerical results are presented in terms of contours of streamlines, isotherms and iso-concentrations as well as the average, local of Nusselt and Sherwood number at the heated wall. The wide ranges of the governing parameter are selected. Here, the Rayleigh Ra number ($10^3 \le \mathrm{Ra} \le 10^6$), the porous layer thickness ($0.3 \le L_p \le 0.05$) and fixing parameters Ra = 10^5, Darcy number $\mathrm{Da} = 10^{-3}$, $L_p = 0.05$, ratio buoyancy Nr, Lewis number Le, Brownian motion Nb, thermopheresis parameter Nt , Nr = Le = Nb = Nt = 0.1.

4.1. EFFECT OF RAYLEIGH NUMBER

Figure.4 presents the effect of the Rayleigh number on the streamlines, isotherms and iso-concentrations. The Rayleigh number varies from 10^3 to 10^6, at low value of Rayleigh number ($\mathrm{Ra} = 10^3$), a single cell circulation is at center of cavity, rotates in clockwise direction, which explains that conduction dominates the flow, at $\mathrm{Ra} = 10^4$, a cell circulation covers the majority of the cavity and increases in intensity, with a low penetration through the porous layer.
At $\mathrm{Ra} = 10^5$, the cell elongates horizontally, forming two poles. At highest Rayleigh number, $\mathrm{Ra} = 10^6$, the two poles extend horizontally, the nanofluid penetrates in the porous layer.

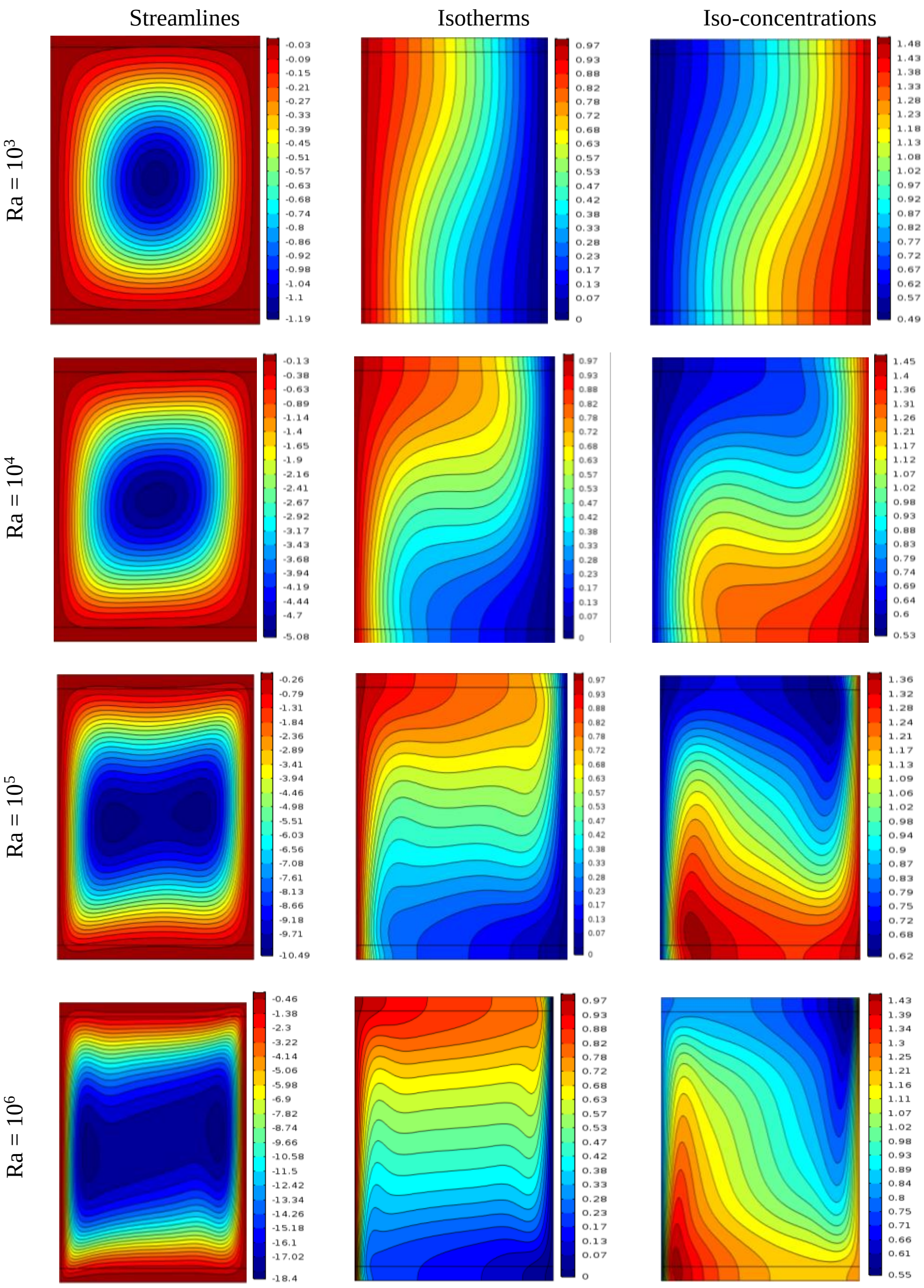

Fig. 4 – Variation of Ra on streamlines, isotherms and isoconentration,
L_p = 0.05, Da = 10^{-3}, Le = Nr = Nb = Nt = 0.1.

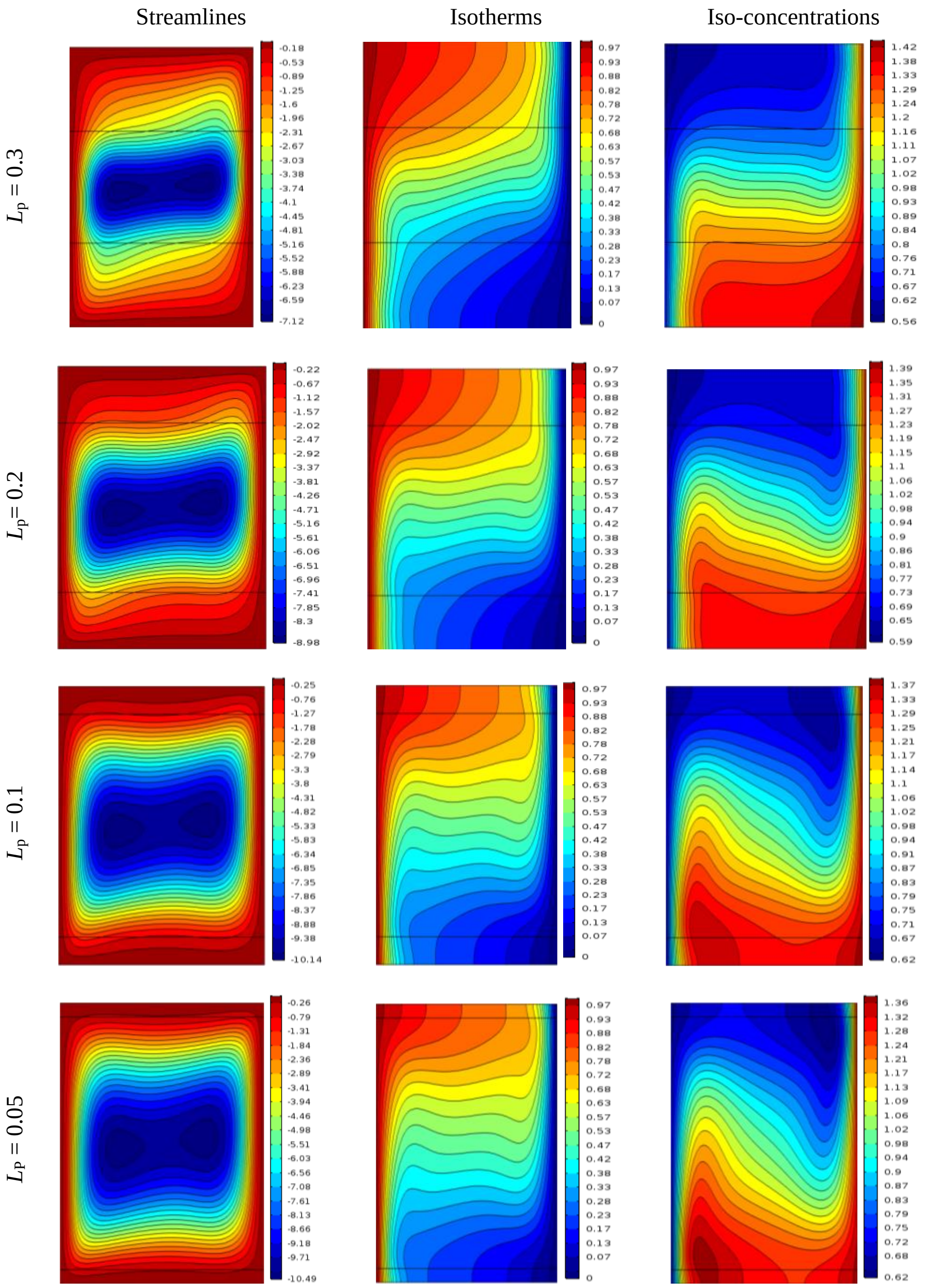

Fig. 5 – Variation of Lp on streamlines, isotherms and isoconentration ,
Ra = 10^5, Da = 10^{-3}, Le = Nr = Nb = Nt = 0.1.

So increasing Rayleigh number increase the strength of streamlines, due to the high buoyancy forces which enhance the convective heat transfer rate.

The isotherms are almost parallel to the vertical walls at $\mathrm{Ra}=10^3$, indicating that the heat transfer is conductive, from $\mathrm{Ra}=10^4$ to 10^5, isotherms are modified due to the augmentation of temperature gradient. At Ra = $10^{6,}$ isotherms become denser to the hot left wall. The flow passes from conductive to convective mechanism and enhances heat transfer in the both layers.

The iso-concentration are affected by increasing Rayleigh number, at $\mathrm{Ra}=10^3$, iso-concentrations are almost parallel to the walls.at $\mathrm{Ra}=10^4$, a stratification of iso-concentrations is observed at bottom cavity. These stratification becomes important at the left hot wall and at bottom cavity at $\mathrm{Ra}=10^5$.

We observe at $\mathrm{Ra}=10^6$, a high nanoparticle concentration at the left corner wall, which signifies important convective heat transfer.

4.2. EFFECT OF THE POROUS LAYER THICKNESS

Figure 5 shows the streamlines, isotherms and iso-concentrations for different values of the porous layer thickness L_p. It is clear that the given parameter ranges from L_p = 0.3 to 0.05.

When we decrease porous layer thickness, we observe that two cells circulation are formed in the middle of the cavity. The intensity cell circulation is strong in nanofluid layer but it is weakened in the porous layer. A low penetration of nanofluid in the porous layer occur especially at L_p = 0.05.

We can interpret this phenomena by less hydrodynamic resistance of porous medium and nanofluids circulate without difficulty in the cavity. The enhancement of convective heat transfer reaches its maximum at L_p = 0.05.

The variation of porous layer thickness from 0.3 to 0.05, shows that the isotherms profiles are diagonal in the porous layer, indicating the domination of the convective heat transfer while, by decreasing the porous layer thickness L_p, the convective heat transfer leads to mainly horizontal isotherms in the nanofluid layer and it becomes very denser to the vertical left hot wall.

The iso-concentrations contours are stratified at the bottom of the cavity and especially from L_p = 0.1 to 0.05 at the left corner wall extremely. The zone stratification indicates that the heat transfer is dominated by the convection mode.

4. 3. CALCULATING OF AVERAGE, LOCAL NUSSELT AND SHERWOOD NUMBERS

4.3.1. Impact of Rayleigh number

Figures 6a and b illustrates the evolution of average Nusselt and Sherwood number with variation of Rayleigh number ($\mathrm{Ra}=10^3$, 10^6).

We observe an increase of Nu_{avg} and Sh_{avg} with Rayleigh number from $Ra = 10^3$ to 10^6.

We constate that the increase of Ra enhances convective heat and mass transfer due to the high gradient temperature which augments thermal buoyancy forces and favors maximum heat transfer particularly at $Ra = 10^6$.

We notice that the local Nusselt and Sherwood numbers increase with Rayleigh number for maximal value of $Ra = 10^6$, on other hand, a slight increase of Nu_{loc} and Sh_{loc} are marked from $Ra = 10^3$ to 10^4 because the presence of nanoparticles, these increase is not noticeable due to the low temperature gradients which explain that conduction dominates flow.

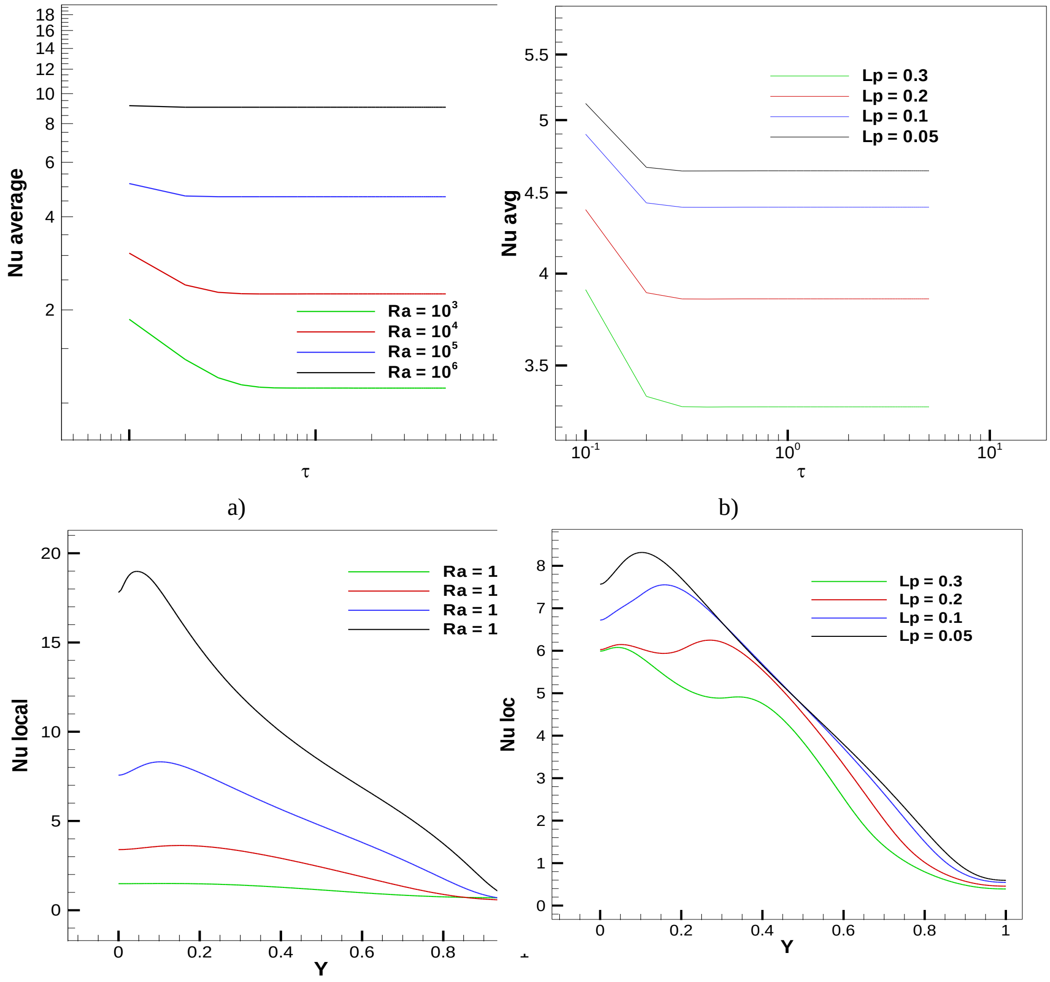

a) b)

c) d)

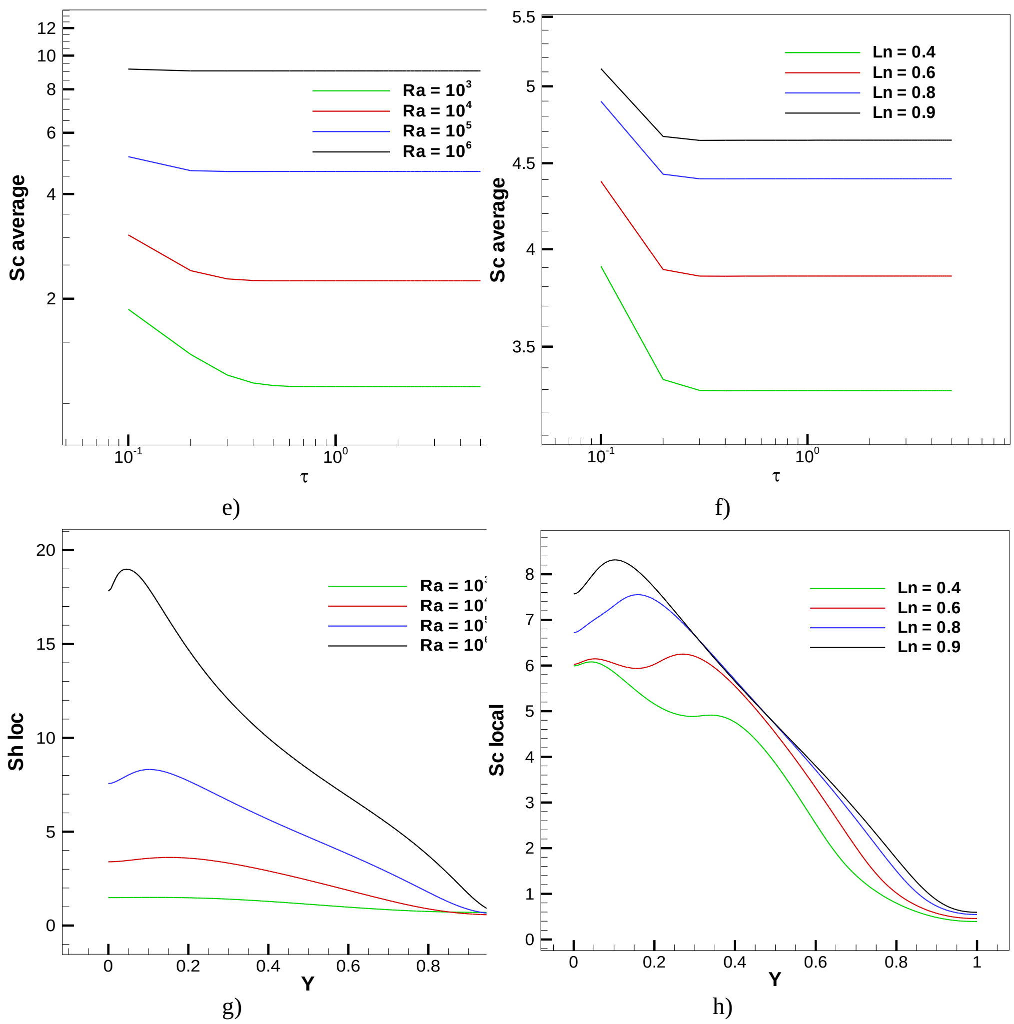

Fig. 6 – Average an Local of Nusselt and Sherwood numbers with the variation of L_p.

A high value of local Nu $_{loc}$ and Sh $_{loc}$ is obtained for $Ra = 10^5$ and 10^6, the Rayleigh number contributes to enhance heat and mass transfer and consequently convection dominates the flow.

4.3.2. Impact of porous layer thickness

Figure 6 shows the variation of average Nusselt and Sherwood numbers with porous layer thickness L_p from 0.3 to 0.05.

We notice in Fig. 6e and f that the average Nusselt number Nu_{avg} and Sh_{avg} increase by reducing the porous layer thickness L_p from 0,3 to 0,05 ,the heat and mass transfer augments and convection dominates the flow.

The nanofluid portion has greater space in the cavity which allows the circulation of nanofluid freely. We conclude that the reduce of the porous layer thickness has an increasing effect on the heat transfer.

Figures 6g and h shows the effects of various values of porous layer thickness at vertical hot left on local Nusslet number Nu_{loc} and Sh_{loc} along the *Y* coordinates.

From L_p = 0.3 to 0.2, a slight increase of Nu_{loc} and Sh_{loc} is observed, continues to increase from 0.2 to 0.1 and 0.05. It is observed that the maximum values of Nu_{loc} and Sh_{loc} are located at the bottom of the hot left wall and decrease towards the top of the wall, Then the Nu_{loc} increases. Afterwards the values tend to fall to a minimum. Furthermore, by decreasing porous layer thickness L_p, a considerable increase of heat transfer and mass rate due of the reduce of hydrodynamic resistance of porous medium and consequently the increase of convective heat transfer.

5. CONCLUSION

The study of natural convection in a square cavity partially filled with a nanofluid and porous medium is investigated numerically using the Buongiorno model. Main attention concerning the effects of the Rayleigh number, and porous layer thickness, on the distribution of dynamic and thermal fields revel the following result:

–The increase of the Rayleigh number causes increased heat transfer and reinforce movement nanofluid in the cavity,

–The reduce of porous layer thickness causes intensity of the nanofluid circulation and leads to enhance heat transfer in the cavity,

–The heat and mass transfer is improved by increasing Rayleigh number and decreasing of porous layer thickness.

6. NOMENCLATURE

B – thermal expansion coefficient (K^{-1})
C – concentration in dimensional form
C_p – specific heat ($Jkg^{-1}K^{-1}$)
Da – Darcy number
g – gravitational acceleration (ms^{-2})
h – heat transfer coefficient
H – height
k – thermal conductivity ($Wm^{-1}K^{-1}$)
K – permeability (m^{-2})
L_c – characteristic length
Le – Lewis numb
Lp – porous layer thickness
Nb – Brownian motion parameter
Nr – buoyancy ratio number
Nt – thermophoresis parameter

$\mathrm{Nu}_{\mathrm{avg}}$ – average Nusselt number
$\mathrm{Nu}_{\mathrm{loc}}$ – Nusselt number local
p – pressure (Nm^{-2})
P – dimensionless pressure
Pr – Prandtl number
Ra – Rayleigh number
$\mathrm{Sh}_{\mathrm{avg}}$ – average Sherwood number
$\mathrm{Sh}_{\mathrm{loc}}$ – local Sherwood number
T – temperature in dimensional form (K)
u, v – velocity components in dimensional form (ms^{-1})
U, V – dimensionless velocity components
W – heat flux Density (Wm^{-3})
x, y – space coordinates in dimensional form (m)
X, Y – dimensionless space coordinates
ν – kinematic viscosity ($\mathrm{m}^2\mathrm{s}^{-1}$)
ρ – density (kgm^{-3})
α – thermal diffusivity ($\mathrm{m}^2\mathrm{s}^{-1}$)
θ – dimensionless temperature
φ – dimensionless concentrate
p – nanoparticles
nf – nanofluid
μ – dynamic viscosity (kg $\mathrm{m}^{-1}\mathrm{s}^{-1}$)
0 – reference
b – Brownien
f – fluid
n – nanofluid
s – solid
c – cold
h – hot
p – particle

Received on Octomber 19, 2021

REFERENCES

1. ESFAHANI, J, A., BORDBAR, V., *Double diffusive natural convection heat transfer enhancement in a square enclosure using nanofluids*, Journal of Nanotechnology in Engineering and Medicine, **2**, *2*, 2011, DOI: 10.1115/1.4003794.
2. GAROOSI, F., SAFAEI, M. R., DAHARI, M., HOOMAN,K., *Eulerian-Lagrangian analysis of solid particle distribution in an internally heated and cooled air-filled cavity*, Applied Mathematicsand Computation, **250**, pp. 28–46, 2015.
3. MEHDI BAHIRAEI, M. H, HAJBARATI, H., VALADKHANI, M., *A comprehensive review on convective heat transfer of nanofluids in porous media: Energy-related and thermohydraulic characteristics*, Applied Thermal Engineering, **178**, September 2020, 115487, https://doi.org/10.1016/j.applthermaleng.2020.115487.
4. ALSABERY, A., SALEH, H, HASHIM, I., *Unsteady natural convection in a square cavity partially filled with porous media using a thermal non-equilibrium model*, International Journal of Mathematical, Computational, Physical, Electrical and Computer Engineering, 2015.
5. BENNACER, R., BEJI, H., MOHAMAD, A., *Double diffusive convection in a vertical enclosure inserted with two saturated porous layers confining a fluid layer*, **42**, *2*, pp. 141–151, 2003.
6. GOYEAU, B., GOBIN, D., *Heat transfer by thermosolutal natural convection in a vertical composite fluid–porous cavity*, Int. Comm. Heat Mass Transfer, **26**, pp. 1115–1126, 1999.
7. BAGCHI, A., KULACKI, F, A., *Experimental study of natural convection in fluid superposed porous layers heated locally from below*, Int. J. Heat Mass Transfer, **55**, pp. 1149–1153, 2012.

8. BAGCHI, A., KULACKI, F, A., *Natural convection in fluid–superposed porous layers heated locally from below*, Int. J. Heat Mass Transfer, **54**, *15–16*, pp. 3672–3682, 2011.
9. LOPEZ, J., J., TAPIA, J., A., *A study of buoyancy driven flow in a confined fluid overlying porous layer*, Int. J. Heat Mass Transfer, **44**, pp. 4725–4736, 2001.
10. AGUILAR-MADERA ,C., G., VALDE´S-PARADA, F., J., GOYEAU, B., OCHOA-TAPIA, J., A., *One-domain approach for heat transfer between a porous medium and a fluid*, Int. J. Heat Mass Transfer, **54**, *9–10*, pp. 2089–2099, 2011.
11. ABU-HIJLEH, B., A., AL-NIMR, M., *A the effect of the local inertial term on the fluid flowin channels partially filled with porous material*, Int. J. Heat MassTransfer, **44**, *8*, pp. 1565–1572, 2001.
12. CARR, M., STRAUGHAN, B., *Penetrative convection in a fluid overlying a porous layer*, Adv. Water Resour., **26**, pp. 263–276, 2003.
13. ALSABERY, A, I., CHAMKHA, A, J., SALEH, H., HASHIM, I., *Natural convection flow of a nanofluid in an inclined square enclosure partially filled with a porous medium*, Scientific Reports , **7**, art. 2357, 2017, DOI:10.1038/s41598-017-02241-x.
14. ALSABERY, A, I., CHAMKHA, A, J., SALEH, H., HASHIM, I., CHANAN, B., *Darcian natural convection in an inclined trapezoidal cavity partly filled with a porous layer and partly with a nanofluid layer*, Sains Malaysiana, **46**, *5*, pp. 803–815, 2017, http://dx.doi.org/10.17576/jsm-2017-4605-15.
15. ZEHBA, A., R., AMMAR, A., ABDELRAHEEM, M., A., ISHAK, H., *Energy and entropy production of nanofluid within an annulus partly saturated by a porous region*, Entropy, **23**, 10, 1237, 2021, https://doi.org/10.3390/e23101237.
16. MUNEER, I., HASSAN, G., *Double diffusive natural convection in a partially layered cavity with inner solid conductive body*, Published on 30 August 2017, Physics Scientia Iranica, DOI:10.24200/SCI.2017.4349.
17. POULIKAKOS, D., BEJAN, A., *Natural convection in vertically and horizontally layered porous media heated from the side*, International Journal of Heat and Mass Transfer, **26**, pp. 1805–1814, 1983.
18. BASIL MAHDI AL-SRAYYIH, SHIAN GAO, SALAM HADI HUSSAIN, *Natural convection flow of a hybrid nanofluid in a square enclosure partially filled with a porous medium using a thermal non-equilibrium model*, Physics of Fluids, **31**, *4*, 043609, 2019, https://doi.org/10.1063/1.5080671.
19. HASSAN, A., A., ISMAEL, M., A., *Mixed convection in superposed nanofluid and porous layers inside lid-driven square cavity*, Int. J. of Thermal & Environmental Engineering, **10**, *2*, pp. 93–104, 2015.
20. ISMAEL, M., A., CHAMKHA, A, J., *Conjugate natural convection in a differentially heated composite enclosure filled with a nanofluid*, Journal of Porous Media, **18**, 7, pp. 699–716, 2015.
21. ARMAGHANI, T., ISMAEL, M., A., CHAMKHA, A, J., *Analysis of entropy generation and natural convection in an inclined partially porous layered cavity filled with a nanofluid*, Journal of Physics, **95**, *3*, 2016, https://doi.org/10.1139/cjp-2016-0570.
22. ARPINO, F., CAROTENUTO, M., CICCOLELLA, M., CORTELLESSA, G., MASSAROTTI, N., MAURO, A., *Transient natural convection in partially porous vertical annuli*, International Journal of Heat and Technology, **34**, *2*, pp. S512–S518, 2016, DOI: https://doi.org/10.18280/ijht.34S245.
23. KADHIM, H, T., JABBAR, F., A., KADHIM, A., A., JABER, A., K., *Numerical study of nanofluid flow in a square cavity with porous medium using a sinusoidal interface*, 4th Scientific International Conference Najaf (SICN), 2019, DOI: 10.1109/SICN47020.2019.9019375.
24. LE BRETON, P., CALTAGIRONE, J, P., ARQUIS, E., *Natural convection in a square cavity with thin porous layers on its vertical walls*, J. Heat Transfer, **113**, *4*, pp. 892–898, 1991, https://doi.org/10.1115/1.2911218.

25. CHAMKHA, A., J., SAZEGAR, S., JAMESAHAR, E., GHALAMBAZ, M., *Thermal non-equilibrium heat transfer modeling of hybrid nanofluids in a structure composed of the layers of solid and porous media and free nanofluids*, Energies, **12**, 3, pp. 1–27, 2019, https://doi.org/10.3390/en12030541.
26. GHALAMBAZ, M., SABOUR, M., POP, I., *Free convection in a square cavity filled by a porous medium saturated by a nanofluid: Viscous dissipation and radiation effects*, Engineering Science and Technology, an International Journal, **19**, *3*, pp. 1244–1253, 2016, https://doi.org/10.1016/j.jestch.2016.02.006.
27. TOOSI, M., H., SIAVASHI, M., *Two-phase mixture numerical simulation of natural convection of nanofluid flow in a cavity partially filled with porous media to enhance heat transfer*, Journal of Molecular Liquids, **238**, pp. 553–569, 2017, https://doi.org/10.1016/j.molliq.2017.05.015.
28. SHEIKHZADEH, G., A., NAZARI, S., *Numerical study of natural convection in a square cavity filled with a porous medium saturated with nanofluid*, Trans. Phenom. Nano Micro Scales, **1**, *2*, pp. 138–146, 2013, DOI: 10.7508/tpnms.2013.02.007.